Ingeniare. Revista Chilena de Ingeniería
ISSN: 0718-3291
facing@uta.cl
Universidad de Tarapacá
Chile

Molina Vicuña, Cristián
Vibration characteristics of single-stage planetary gear transmissions
Ingeniare. Revista Chilena de Ingeniería, vol. 22, núm. 1, enero, 2014, pp. 88-98
Universidad de Tarapacá
Arica, Chile

Vibration characteristics of single-stage planetary gear transmissions

Características vibratorias de transmisiones planetarias de una etapa

Cristián Molina Vicuña[1]

Recibido 8 de marzo de 2011, aceptado 17 de junio de 2013
Received: March 8, 2011 Accepted: June 17, 2013

RESUMEN

En su aplicación a transmisiones planetarias, el monitoreo de condiciones basado en el análisis de vibraciones no ha otorgado resultados favorables. Una de las principales causas es la inadecuada interpretación del espectro de las vibraciones. La estructura de las líneas presentes en el espectro de las vibraciones medidas en la parte externa del anillo de una transmisión planetaria sin fallas, está estrechamente relacionada con la geometría de la transmisión. Por esta razón, es posible encontrar distintas estructuras espectrales para distintas transmisiones planetarias. Para explicar este fenómeno, en este trabajo se presenta un modelo de las vibraciones para una transmisión planetaria de una etapa. El modelo es realizado en el dominio tiempo, y analizado en el dominio frecuencia mediante el uso de la transformada de Fourier. Se muestra que algunas transmisiones planetarias con distintas geometrías presentan estructuras espectrales similares. Basado en esto, se propone una clasificación de las transmisiones planetarias en cuatro grupos, presentándose las características del espectro de cada uno de ellos. La clasificación propuesta permite una rápida estimación de la estructura del espectro esperado de las vibraciones de cualquier transmisión planetaria de una etapa. De esta forma, se espera contribuir a mejorar los resultados del monitoreo de condiciones en transmisiones planetarias.

Palabras clave: Vibraciones, transmisión planetaria, diagnóstico de fallas, análisis de vibraciones, monitoreo de condición.

ABSTRACT

Condition monitoring based on vibration measurement and analysis of planetary gear transmissions has not provided the same good results observed in conventional fixed-shaft gear transmissions. One of the causes being the improper interpretation of the vibration spectrum. The structure of the lines present in the spectrum of the vibrations measured on a non-faulty planetary gear transmission, with a sensor mounted on the outer part of the ring gear, is strictly related to the geometry of the transmission. Hence, different spectral patterns can be found for different planetary gear transmissions. In this work, a vibration model for a single-stage planetary gear transmission is presented to explain this phenomenon. The model is developed in the time domain and analyzed in the frequency domain by using the Fourier transform. It is shown that some planetary gear transmissions, with different geometries, present similar spectral structures. Based on this, a classification of planetary gear transmissions in four groups is proposed. The spectral characteristics of the vibrations of each group are presented. The classification allows for a fast estimation of the expected spectral pattern of the vibrations of any single-stage planetary gear transmission. Through this, contribution is expected in order to increase the effectiveness of vibration-based condition monitoring in planetary gear transmissions.

Keywords: Vibrations, planetary gear transmission, fault diagnostic, vibration analysis, condition monitoring.

[1] Laboratorio de Vibraciones Mecánicas. Departamento de Ingeniería Mecánica. Universidad de Concepción. Edmundo Larenas 270 int. Concepción, Chile. E-mail: crimolin@udec.cl

LIST OF SYMBOLS

$a_i(t)$:	Amplitude modulation function of planet gear i
$a_{q\in Z}$:	Fourier coefficients of $a_i(t)$
f_C:	Frequency of rotation of the carrier plate
f_g:	Gear mesh frequency
i:	Planet gear index
m:	Integer number
N:	Total number of planet gears
t_i:	Time-shift due to the relative position of planet gear i with respect to planet gear 1
t_1:	Time-shift due to the unknown position of planet gear 1 at measurement start
$v_i(t)$:	Vibration generated by the meshing of the i-th planet gear with the ring gear
$v_{k\in Z}$:	Fourier coefficients of $v_1(t)$
$x(t)$:	Vibration measured by the sensor
$X(f)$:	Fourier transform of $x(t)$
$x_i(t)$:	Amplitude modulated vibration of planet gear i
Z_p:	Number of teeth of the planet gear
Z_R:	Number of teeth of the ring gear
Z_S:	Number of teeth of the sun gear
γ_i:	Phase-shift of $v_i(t)$ with respect to $v_1(t)$
$\delta(f)$:	$\delta(f) = 1$, if $f = 0$; and $\delta(f) = 0$, if $f \neq 0$
Δf:	Frequency resolution
θ_1:	Unknown angular position of planet gear 1 at measurement start
φ_i:	Angular position of planet gear i with respect to planet 1

INTRODUCTION

Planetary gear transmissions are used in a large diversity of machines within the industry. Particularly, they are used when high power transmission is required [1]. Machines working with high power levels are typically considered critical within the process. Therefore, they receive special attention aiming to avoid unexpected failures that might need to stop the operation of the machine for repairing, thus hindering or even completely stopping the whole production. Typically, a condition monitoring strategy is used in these types of machines. Within this strategy, the vibration measurement and analysis appears as the most powerful tool for early failure diagnosis. In order to prevent their development into major damages, the development of the detected failures is watched carefully. In parallel, repair activities are scheduled to optimize resources and minimize the time the machine remains out of production.

Vibration-based failure diagnosis has been an active field of research for decades [2]. Consequently, several techniques based on different signal processing tools have been developed, leading to an increase in the diagnosis capabilities of many failure types on different machine parts. In the case of gear failures, the interest has been mainly focused on conventional (fixed-shaft) gear transmissions, where satisfactory results have been obtained [3-4]. Conversely, planetary gear transmissions have not been addressed with the same interest and the results of failure diagnosis on these units has not been as favorable as in the case of fixed-shaft gear transmissions [5-6].

Considering that planetary gear transmissions are used in critical machines, and that the results of the condition monitoring strategies used in planetary gear transmissions have not produced favorable results, the problem becomes evident. We believe that one of the major reasons for the unfavorable results of the vibration-based condition monitoring strategy used in planetary gear transmissions relies on the insufficient knowledge about the characteristics of their vibrations. Regarding the spectral analysis of vibrations performed in the industry, the author has observed that planetary gear transmissions are erroneously considered as if they were fixed-shaft transmissions, even though the distinction has been made in the literature [7]. As shown in this work, vibrations generated in different planetary gear transmissions can produce spectra with different structures. This is in opposition to the case of fixed-shaft gear transmissions, were roughly the same structure is always found. Hence, planetary gear transmissions should be treated differently. Moreover, when analyzing the vibration spectrum of a planetary gear transmission, the expected structure of the vibrations (i.e. the *spectral pattern*) should be previously known. This is only possible if a previous knowledge of the vibrations generated in these units exists.

The main objectives of this paper are (i) to provide the reader a clear overview of the vibrations generated in a single-stage planetary gear transmission, and (ii) to provide the theoretical background to sustain

a classification of planetary gearboxes according to the spectral structure of their vibrations. A validation of the model is also presented, based on the comparison with real measurements. All this should allow the a-priori determination of the structure of the vibration spectrum of any single-stage planetary gear transmission.

MODEL DESCRIPTION

If the tooth profiles of a gear transmission were perfect involutes and the teeth were non-deformable, then no vibration would be generated due to the tooth gear meshing process of geared transmissions. This, however, does not occur. In the reality, tooth profiles differ from the perfect involute due to, for example, fabrication errors, deformation under load, wear, etc. Consequently, vibrations resulting from tooth meshing are inherent to geared transmissions.

The transmission error (TE) is a measurable function, which quantifies the deviations of the real tooth profiles from perfect involutes. Accordingly, it has been traditionally recognized as the cause of vibrations generated in geared transmissions [1, 8]. Due to the meshing of successive pairs of teeth from the conducted and conduced gear wheels, the TE is a periodic function with a period equal to the inverse of the gear mesh frequency (i.e. the frequency with which successive pairs of meshing teeth come into contact) [9]. Consequently, the typical spectrum (i.e. spectral pattern) of the vibrations measured on a non-faulty fixed-shaft gear transmission presents lines at the gear mesh frequency f_g and harmonics (Figure 1). Also spectral lines at the rotational frequency of each geared wheel are usually present in the spectrum, as well as sidebands spaced at these frequencies around the gear mesh frequency and harmonics. This spectral pattern represents the normal spectrum of the vibrations measured on any fixed-shaft gear transmission, varying only the absolute and relative amplitude of the spectral lines, as well as their frequencies, which are related to the rotational frequency of the gear wheels. In the case of planetary gear transmissions, different structures of the vibration spectrum can be found, thus making impossible the definition of a unique spectral pattern. In what follows, we present a model for the vibrations generated in a planetary gear transmission to explain the cause of this phenomenon. It must be pointed out that the model presented here is similar to other models found in the literature [7, 10]. However, the frequency analysis of the model, which determines the shape of the spectrum, is obtained using the analytical Fourier theory, rather than based on results from numerical simulations. This has the advantage of giving the reader a clearer overview of the phenomena that produces different spectral structures on planetary transmissions.

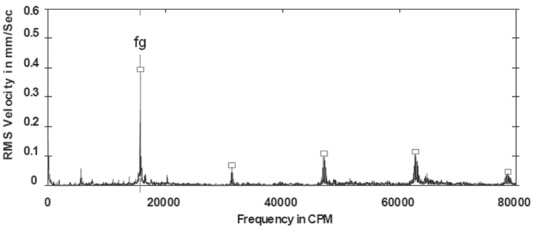

Figure 1. Typical vibration spectrum of fixed-shaft gear transmissions.

A single-stage planetary gear transmission consists of one central gear –called the sun gear—that meshes with one or more intermediate gears –called the planet gears—placed at different angular positions around the central gear. The intermediate gears are held in their position by a structure called the carrier plate. Additionally, the intermediate gears mesh with an outer gear called the ring gear. Figure 2 shows a cross-sectional view of a single-stage planetary gear transmission. In a planetary gear transmission, the ring gear remains fixed during operation. When used in speed-reduction mode, the input of the transmission is the sun gear. As the sun gear rotates, the planet gears are forced to rotate around their own axis of rotation. However, since they additionally mesh with the fixed ring gear, they are also forced to revolve around the axis of rotation of the sun gear. The revolving

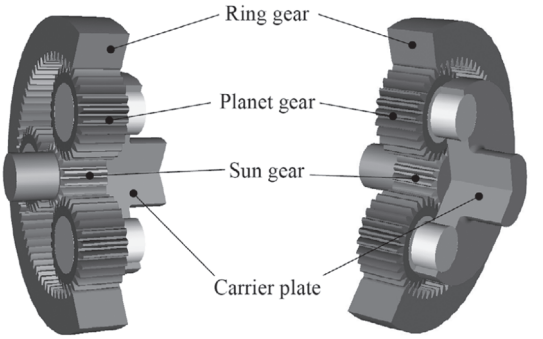

Figure 2. Illustration of a single-stage planetary gear transmission.

motion of the planet gears is finally transferred to the carrier plate, which constitutes the output of the transmission. When used in speed-increasing mode, the functioning is the opposite.

Planetary gear transmissions usually form part of larger transmissions. For this reason, their bearing housings are inaccessible. Therefore, the vibrations are typically measured in the outer part of the ring gear [7], as represented in Figure 3. Consequently, the model is developed to represent this situation. The following considerations are taken in the development of the model: (i) vibrations are only generated in the planet-ring gear mesh processes; (ii) the vibrations generated in each planet-ring gear mesh process are periodic, have the same amplitude and have no amplitude modulation; and (iii) the vibrations are transmitted to the sensor through the ring gear only. Reference [11] addresses the relaxation of these considerations.

Figure 4 shows the vibrations $v_{i=1\ldots N}(t)$ generated in the gear mesh processes between each planet i and the ring gear, as experienced by an observer standing on and rotating with the carrier plate. Here, the symbol i is used to represent the index of the planet gear (i.e. $i=1\ldots N$, where N is the total number of planet gears present in the transmission). All vibrations $v_{i=1\ldots N}(t)$ have the same shape and share the same gear mesh frequency f_g, which is given by

$$f_g = Z_R f_C \tag{1}$$

where Z_R is the number of teeth of the ring gear and f_C is the rotational frequency of the carrier plate.

Interestingly, as shown in Figure 4, a time-shift can exist between the different vibrations $v_{i=1\ldots N}(t)$. Taking a given point within the line of action of meshing teeth from corresponding gear mesh processes (e.g. the pitch point), this means that the contact at this point for the meshing tooth pair of each gear mesh process can take place at different time instants. The time-shift can also be expressed as a phase-shift. Considering the planet gear No. 1 as the reference planet, the phase-shift between the vibration generated in the gear mesh process of the i-th planet gear with the ring gear and the vibration generated in the gear mesh process of the reference planet gear with the ring can be calculated as follows [11-12].

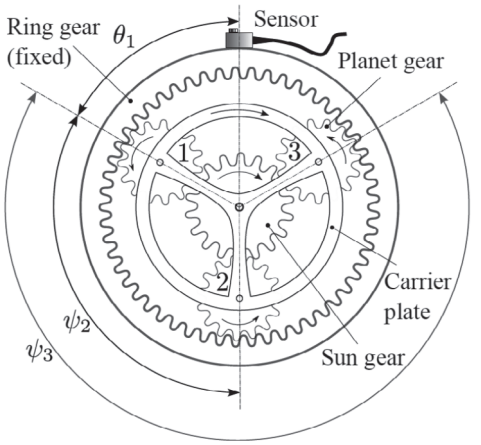

Figure 3. Measurement arrangement.

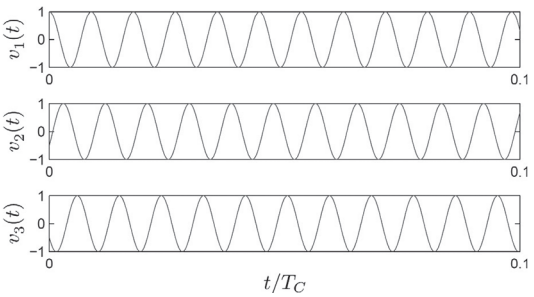

Figure 4. Illustration of $v_{i=1\ldots N}(t)$.

$$\gamma_i = \frac{\varphi_i Z_R}{2\pi} \tag{2}$$

where φ_i is the relative angle between the position of the i-th planet gear and the reference planet gear (Figure 3.) It is clear from equation (2) that the phase-shift magnitude is determined by the geometry of the transmission. Hence, it is a specific feature.

Under consideration of the phase shift presented in equation (2), the vibration $v_i(t)$ can be expressed as a time-shifted version of $v_1(t)$

$$v_i(t) = v_1\left(t - \frac{\gamma_i}{f_g}\right) \tag{3}$$

In addition, during the operation of the transmission, the planet gears revolve around the sun gear. This makes the contact points between each planet gear and the ring gear –i.e. the source location of the vibrations $v_{i=1\ldots N}(t)$—to follow the internal circumference of the ring gear. On the other hand,

the sensor remains steady. Thus, the distance between the sensor and the sources of the vibrations $v_{i=1...N}(t)$ is variable during the operation of the transmission. The variable distance produces a variable transmission path, which has an amplitude modulation effect on the vibrations $v_{i=1...N}(t)$. Hence, the sensor experiences an increase in the amplitude of the vibration $v_i(t)$ as the i-th planet gear approaches the sensor position; conversely, it experiences a decrease in the amplitude of the vibration, as the planet gear moves farther away. As illustrated in Figure 5, this process repeats with each rotation of the carrier plate, because the planet gears rotate together with this structure. Consequently, the amplitude modulation function $a_i(t)$ due to the variable transmission path is a periodic function with fundamental frequency equal to the rotational frequency of the carrier plate f_C.

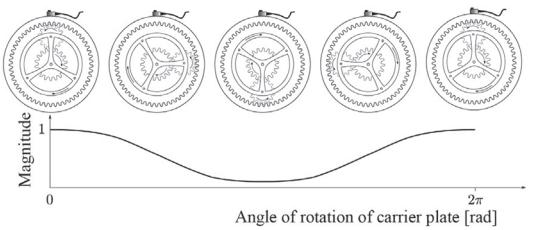

Figure 5. Amplitude modulation effect due to the variable transmission path.

Furthermore, since all vibrations $v_{i=1...N}(t)$ are transmitted to the sensor through the ring gear, the amplitude modulation function $a_i(t)$ of the vibration generated on the i-th planet gear $v_i(t)$, can be expressed in terms of the amplitude modulation function $a_i(t)$ of the vibration generated in the reference planet gear

$$a_i(t) = a_1\left(t - \frac{\varphi_i}{2\pi f_C}\right) \tag{4}$$

Figure 6 shows schematically the shape of the amplitude modulation functions for each gear mesh process.

With the definitions presented above, the expression of the vibration generated in the gear mesh process between the i-th planet gear and the ring gear as measured by the sensor can be written as

$$x_i(t) = a_i(t)v_i(t) \tag{5}$$

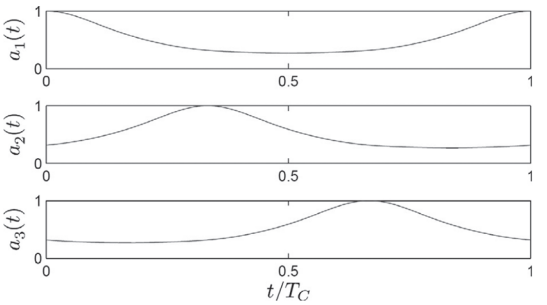

Figure 6. Illustration of the amplitude modulation functions $a_{i=1...N}(t)$, according to equation (4).

Figure 7 illustrates $x_i(t)$ for $i = 1...N$, according to equation (5).

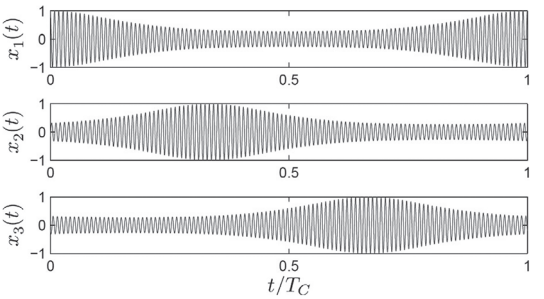

Figure 7. Illustration of $x_{i=1...N}(t)$, according to equation (5).

Since all vibrations $v_{i=1...N}(t)$ occur simultaneously, and considering the system as linear, the total vibration $x(t)$ experienced by the sensor is the sum of all amplitude-modulated vibrations $x_{i=1...N}(t)$

$$\begin{aligned} x(t) &= \sum_{i=1}^{N} x_i(t) = \sum_{i=1}^{N} a_i(t)x_i(t) \\ &= \sum_{i=1}^{N} a_1\left(t - \frac{\varphi i}{2\pi f_C}\right) v_1\left(t - \frac{\gamma_i}{f_g}\right) \end{aligned} \tag{6}$$

Equation (6), which is illustrated in Figure 8, represents a model for the vibrations generated in a single-stage planetary gear transmission, when measured according to Figure 3.

It must be pointed out that equation (6) assumes the reference planet is at the sensor position at the measurement start. Logically, this is only a particular case. The model can be generalized to an unknown position at the measurement start, by

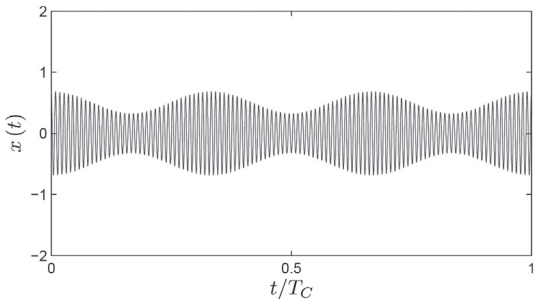

Figure 8. Illustration of $x(t)$, according to equation (6).

including a time-shift $t_1=\theta_1/(2\pi f_C)$ into the amplitude modulation function $a_1(t)$, where θ_1 represents the unknown angular position of the reference planet gear at the measurement start (Figure 3). Thus, the generalized expression of the model is

$$x(t)=\sum_{i=1}^{N} a_1(t-t_1-t_i)\,v_1\left(t-\frac{\gamma_i}{f_g}\right) \tag{7}$$

where $t_i=\varphi_i/2\pi f_C$. It can also be shown that the term γ_i/f_g in equation (7) is equivalent to t_i. That is, both functions $a_1(\cdot)$ And $v_1(\cdot)$ are affected by the same amount of time shift.

FREQUENCY ANALISYS: STRUCTURE OF THE VIBRATION SPECTRUM

The spectrum of a vibration signal is a graphic representation of the coefficients of the Fourier transform of the signal, and is used for the examination of its frequency content. The vibration spectrum and its proper interpretation constitute the fundamental technique for vibration-based failure diagnosis of rotating machines. Logically, a proper interpretation is only possible if there is a previous knowledge about the spectral structure of the vibrations of the mechanical system under analysis. In this section, we present the results from the frequency analysis of the vibrations generated on a single-stage planetary gear transmission and the structure of the vibration spectrum for the non-faulty condition. The procedure is based on the theoretical determination of the Fourier transform of the model presented in equation (7) and its analysis for planetary gear transmissions with different geometries.

The Fourier transform of $x(t)$ is given by [11]

$$X(f)=F\{x(t)\}=\sum_{i=1}^{N} F\{a_i(t)\}*F\{v_i(t)\} \tag{8}$$

where $F\{\cdot\}$ represents the Fourier transform and * denotes the convolution product (i.e. $a(x)*b(x)=\int_R a(x-X)\,b(X)\,dX$).

Recalling that $a_i(t)$ was defined as a periodic function, it accepts Fourier series decomposition

$$a_i(t)=a_1\left(t-t_1-\frac{\varphi i}{2\pi f_C}\right)=\sum_{q\in Z} a_q e^{j2\pi q f_C\left(t-t_1-\frac{\varphi_i}{2\pi f_C}\right)} \tag{9}$$

where $a_{q\in Z}$ are the Fourier coefficients of $a_1(t)$. Similarly for $v_i(t)$

$$v_i(t)=v_1\left(t-\frac{\gamma_i}{f_g}\right)=\sum_{k\in Z} v_k e^{j2\pi k f_g\left(t-\frac{\gamma_i}{f_g}\right)} \tag{10}$$

where $v_{k\in Z}$ are the Fourier coefficients of $v_1(t)$.

Hence, the Fourier transforms of $a_i(t)$ and $v_i(t)$ can be calculated from equation (9) and equation (10)

$$F\{a_i(t)\}=\sum_{q\in Z} a_q e^{-j2\pi q f_C\left(t_1+\frac{\varphi_i}{2\pi f_C}\right)}\delta(f-qf_C) \tag{11}$$

$$F\{v_i(t)\}=\sum\nolimits_{k\in Z} v_k e^{-jk\varphi_i Z_R}\delta(f-kf_g) \tag{12}$$

where $\delta(f)=1$, if $f=0$; and $\delta(f)=0$, if $f\neq 0$. Finally, substituting equations (11) and (12) into equation (8) yields

$$X(f)=\sum_{k\in Z}\sum_{q\in Z}\sum_{i=1}^{N} a_q v_k e^{-j2\pi q f_C t_1} e^{-j\varphi_i(kZ_R+q)}\delta(f-kf_g-qf_C) \tag{13}$$

The graphical representation of equation (13) is the frequency spectrum. Please observe that the term $\delta(f-kf_g-qfC)$ in equation (13) implies that $X(f)$ can take non-zero values only for the frequencies $f=kf_g+qf_C$, with $k,\ q\in Z$. Furthermore, the

exponential term $e^{-j\varphi_i(kZ_R+q)}$ determines the phase-shift of the spectral component at the frequency $f=kf_g+qf_C$, due to the gear mesh of the i-th planet gear and the ring gear with respect to the constant phase $2\pi qf_Ct_1$. For example, in the case of planetary gear transmissions with equally-spaced planet gears, $\varphi_i=2\pi(i-1)/N$. Substitution of this expression into the exponential term $e^{-j\varphi_i(kZ_R+q)}$ yields

$$e^{-j\varphi_i(kZ_R+q)} = e^{-j2\pi(i-1)\left[\frac{kZ_R+q}{N}\right]} \tag{14}$$

Note from equation (14) that the exponential term acts as a sampling function, since it can yield non-zero values only for combinations of k and q satisfying the condition $(kZ_R+q)=mN$, where m is an integer number. This observation is in accordance with [13]. Hence, for planetary gear transmissions with equally-spaced planet gears, equation (13) can be written as

$$X(f)=\begin{cases} Na_q v_k e^{-j2\pi qf_Ct_1}, \text{if}(kZ_R+q)/N\in Z \\ 0, \text{otherwise} \end{cases} \tag{15}$$

Note also that the gear mesh frequency is obtained for $k=1$ and $q=0$. It is observed from equation (15) that the spectrum will show a line with non-zero magnitude at this frequency only if the quotient Z_R/N is an integer number. If this condition is not fulfilled, the spectrum will show no line at the gear mesh frequency. Figure 9 shows with thin line a portion of the spectrum around the gear mesh frequency according to equation (15) for a planetary gear transmission with three equally-spaced planets and $Z_R=112$. Note the absence of a non-zero magnitude line at the gear mesh frequency f_g=112 f_C. In the same figure, with a thick gray line, the scaled version of the spectrum of the vibration generated in the gear mesh process of a single planet gear with the ring gear x_i (t) has been plotted. This figure also evidences the sampling effect of the exponential term of equation (14).

From the analysis presented in the preceding paragraphs, it results evident that the geometry of the planetary gear transmission is a determining factor in the spectral structure of the vibrations generated on it. In simple words, planetary gear transmissions with different geometries can originate vibrations with different non-zero lines in their spectrum; however, all representing the normal vibratory behaviour (i.e. non-faulty.) Particular cases have been presented to illustrate this situation [7, 13]. However, it is only recently that the problem of the determination of the spectral structure of the vibration spectrum for the generality of single-stage planetary gear transmissions has been considered. In [10], a vibration model similar to the presented in this work is used. The vibration spectrum is calculated numerically from the model by using the FFT (Fast Fourier Transform) algorithm, for different geometries. The authors found that it was possible to group certain planetary gear transmissions with different geometries, because their vibrations produced spectra with similar structures. Based on this, a classification of planetary gear transmissions in five groups was proposed. The classification was done based in the observation of the spectra obtained numerically from the model; a theoretical justification of the classification was not presented. This was carried out in [11] based on the analysis of the structure of equation (13) for different geometries. Following, the most important results of this analysis are presented.

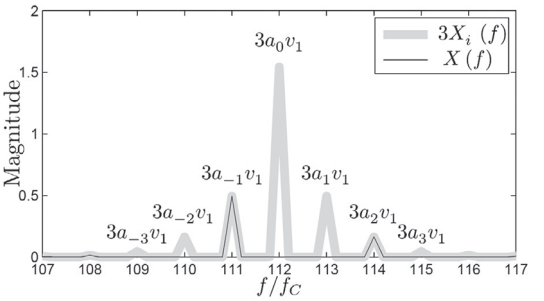

Figure 9. Thin line: spectrum $X(f)$ of the total vibration $x(t)$; thick line: scaled version of the spectrum $X_i(f)$ of the vibration $X_i(t)$.

The first result is related to the classification itself. A new, more general, 4-group classification is proposed [11]:

Group A: Planetary gear transmissions with equally-spaced planet gears and in-phase gear mesh processes;

Group B: Planetary gear transmissions with equally-spaced planet gears and out-of-phase gear mesh processes;

Group C: Planetary gear transmissions with unequally-spaced planet gears and in-phase gear mesh processes; and

Group D: Planetary gear transmissions with unequally-spaced planet gears and out-of-phase gear mesh processes.

where the conditions of planet gear spacing and phase of the gear mesh processes are fully determined by the geometry of the transmission. Hence, provided the geometry is known, it is possible to determine which group the transmission pertains to.

The second result is related to the specific characteristics of the vibration spectra of each group. These are presented in the following subsections.

Group A

This group is formed by planetary gear transmissions whose planet gears are equally distributed around the sun gear. Additionally, the gear mesh processes taking place in the transmission are in-phase, which occurs if $Z_R/N=m$, where m is an integer number.

Figure 10 shows the characteristic vibration spectrum for planetary gear transmissions of group A. The spectrum presents lines at the gear mesh frequency and harmonics. In addition, each of these lines presents a symmetrical distribution of spectral lines, spaced at $\Delta_f=Nf_C$.

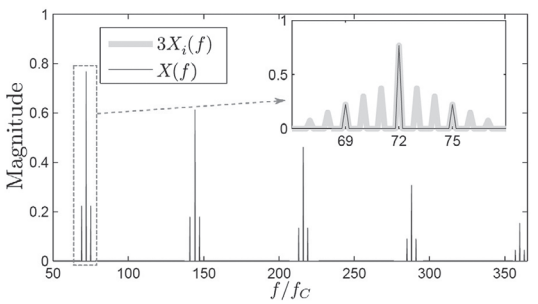

Figure 10. Illustration of the spectrum for a planetary gear transmission of group A ($Z_R=72$ and $N=3$; synthetic data).

Group B

Planetary gear transmissions of this group have planet gears which are equally distributed around the sun gear. Additionally, the gear mesh processes occurring in the transmission are out-of-phase, a condition met if the quotient Z_R/N is a non-integer.

Figure 11 shows the typical vibration spectrum for planetary gear transmissions of group B. In this case, the spectrum presents no line (i.e. it presents a line with zero magnitude) at the gear mesh frequency and harmonics. Additionally, an asymmetrical (in magnitude and frequency) distribution of spectral lines is observed around the frequency axis defined by the gear mesh frequency and its harmonics. Furthermore, the shape of the spectral line distribution around each gear mesh frequency harmonic is different, although the separation between the lines is the same and is equal to $\Delta f=Nf_C$.

In case the N-th harmonic of the gear mesh frequency is present in the vibration, then the spectral line at this frequency will have non-zero magnitude, as illustrated in the upper right inlet of Figure 11. The distribution of lines around this frequency is symmetric in magnitude and frequency.

If $Z_R/N=0.5$, then the lines at the frequencies $N/2$-th harmonics of the gear mesh frequency will have non-zero magnitude, each with a symmetrical distribution of lines spaced at $\Delta_f=Nf_C$.

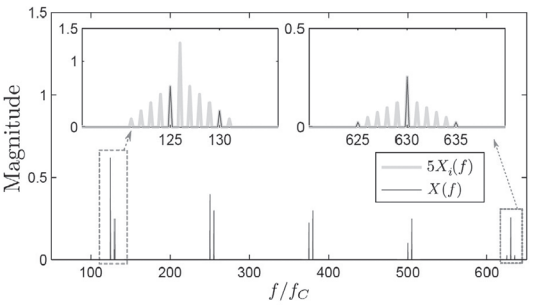

Figure 11. Illustration of the spectrum for a planetary gear transmission of group B ($Z_R=126$ and $N=5$; synthetic data).

Group C

The planet gears are not equally distributed around the sun gear for planetary gear transmissions of this group. In addition, the gear mesh processes occurring in the transmission are in-phase, which holds only if $(\varphi_i Z_R)/(2\pi)=m$, where m is an integer number.

Figure 12 shows the typical vibration spectrum for planetary gear transmissions of this group. For this group, the spectrum presents non-zero magnitude lines at the gear mesh frequency and harmonics. A symmetrical (in amplitude and frequency) distribution of spectral lines is present around each of the axis defined by the gear mesh frequency and

its harmonics. The separation between the lines of the distribution is $\Delta_f = f_C$. Furthermore, the shape of the distribution and the relative magnitude between the central line and the surrounding lines is the same for all harmonics of the gear mesh frequency.

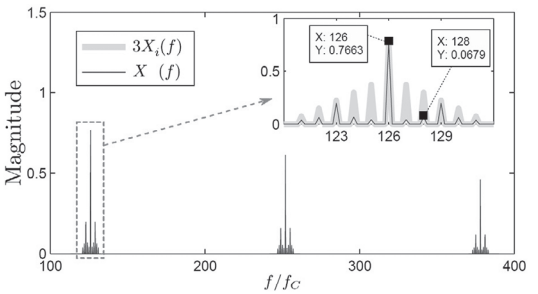

Figure 12. Illustration of the vibration spectrum for a planetary gear transmission of group C ($Z_R = 126$ and $\{\varphi_i\} = \{0^o; 120^o; 220^o\}$; synthetic data).

Group D

This group is composed by planetary gear transmissions whose planet gears are not equally distributed around the sun gear and whose gear mesh processes are out-of-phase. This latter condition is met only if $\varphi_i\, Z_R/(2\pi)$ is non-integer or zero.

It is not possible to typify a defined vibration spectrum structure, because several geometries of planetary gear transmissions meet the above mentioned conditions, each originating a different vibration spectrum structure. Nonetheless, it can be stated that the majority of the transmissions of this group will present a vibration spectrum with non-zero magnitude lines at the gear mesh frequency and harmonics, each with a magnitude-asymmetrical distribution of spectral lines spaced at $\Delta_f = f_C$. Moreover, the relative shape of the spectral line distribution around each harmonic of the gear mesh frequency will be different. These characteristics are illustrated in Figure 13.

COMPARISON WITH REAL MEASUREMENTS

Figure 14 shows the spectrum from a PG pertaining to group A ($Z_R = 72$ and three equally-distributed planet gears.) In this case, lines at the gear mesh frequency and harmonics are observed, as the model predicts (only the portion around f_g is shown.) The

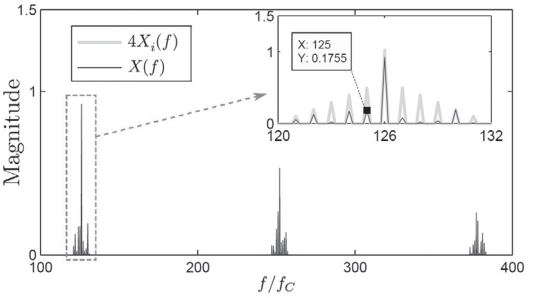

Figure 13. Illustration of the vibration spectrum for a planetary gear transmission of group D ($Z_R = 126$ and $\{\varphi_i\} = \{0^o; 97.2^o; 174.6^o; 282.6^o\}$; synthetic data).

model also predicts the presence sidebands spaced at $3 \times f_C$ around the gear mesh harmonics; these are also observed in the spectrum. Additionally, sidebands spaced at f_C (not predicted by the model) are recognized; their presence could be explained by differences existing in the vibrations generated by the different planets, something not considered in the presented model.

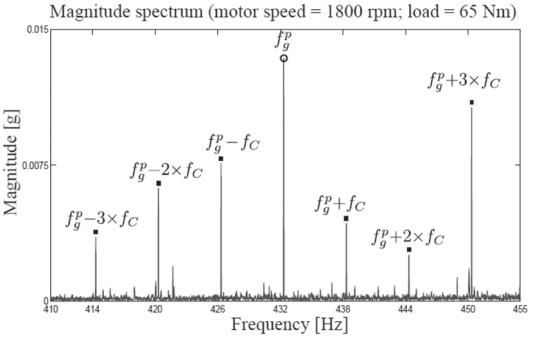

Figure 14. Portion of vibration spectrum around the gear mesh frequency (f_g^p in this figure). Planetary gearbox of group A.

Figure 15 shows another vibration spectrum from a PG pertaining to group A ($Z_R = 99$ and three equally-distributed planet gears.) In this case, the picture is closer to the model prediction. The spectrum is dominated by the lines at the gear mesh frequency and harmonics, each with sidebands spaced at Nf_C ($N = 3$ in this case). The structure of lines around the gear mesh frequency is, however, not symmetric as the model predicts. This can be due to the interaction with the frequency response function of the system, not considered in the model.

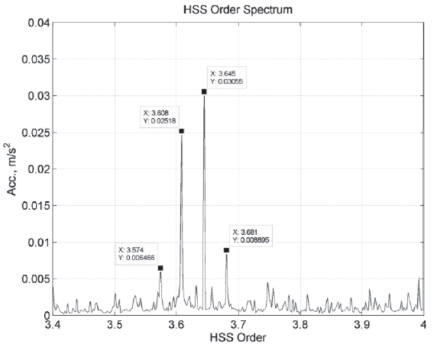

Figure 15. Portion of vibration spectrum around the third multiple of the gear mesh order ($3f_g^p = 3.645$; $f_C = 0.012$). Planetary gearbox of group A [14].

Figure 16 shows the vibration spectrum from a PG pertaining to group B ($Z_R = 81$ and four equally-distributed planet gears.) In this case the line at the gear mesh frequency is (almost) absent. Instead, the dominant component is at $f_g - f_C$, which corresponds to the integer multiple of Nf_C nearest to f_C, all this is in agreement with the model prediction for this group of PG.

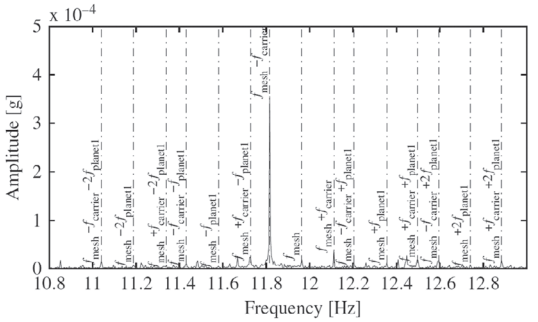

Figure 16. Portion of vibration spectrum around the gear mesh frequency (f_{mesh} in this figure). Planetary gearbox of group B [15].

Figure 17 shows the spectrum of the vibrations measured on another PG of group B ($Z_R = 113$ and three equally-distributed planet gears.) As the model indicates, the lines at the gear mesh frequency ($f_g = 113$ in this case) and its second harmonic are suppressed and, therefore, absent in the spectrum. In this PG, the third multiple of the gear mesh frequency coincides with the harmonic Nf_g, for which a different picture is expected according to the model (see the upper right inlet of Figure 11.) Figure 18 shows the spectral structure around Nf_g.

As predicted by the model, the line at the third multiple of the gear mesh frequency is present in the spectrum, with sidebands spaced at Nf_C. Note the model predicts a symmetrical distribution around this multiple, which is in agreement with this real measurement. This, however, can be different in other cases, due to the influence of the response of the system, as previously mentioned.

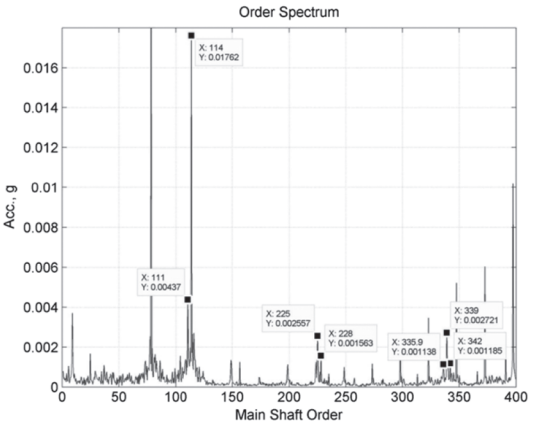

Figure 17. Vibration spectrum of a planetary gearbox of group B [16].

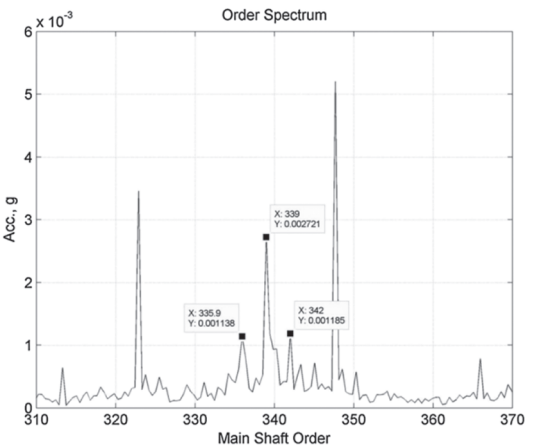

Figure 18. Portion of vibration spectrum around the third multiple of the gear mesh order ($3f_g^p = 339$; $f_C = 1$). Planetary gearbox of group B [16].

CONCLUSIONS

A model descriptive of the vibrations measured in the outer part of the ring gear of a single-stage planetary gear transmission has been presented. From the frequency analysis of the model it is concluded that

the lines present in the spectrum of the measured vibrations are determined by the geometry of the transmission. Hence, the structure of the vibration spectrum can vary significantly for different planetary gear transmissions, although all represent their normal vibratory behaviour. Based on the analytical study of the expected vibration spectrum structure for different geometries, a classification of planetary gear transmissions in four groups is proposed. The characteristics of the spectrum of each group have been presented. This allows the a-priori estimation of the vibration spectrum structure of a non-faulty single-stage planetary gear transmission, provided the geometry of the transmission is known. The results from the model find good agreement with the observation from real measurements.

ACKNOWLEDGMENTS

The author would like to thank FONDECYT for the support of project 11110017.

REFERENCES

[1] J.D. Smith. "Gear Noise and vibration". Marcel Dekker. 2nd Edition. New York, USA. 2003.

[2] J.P. Den Hartog. "Mechanical vibrations". McGraw-Hill. 4th Edition. USA. 1956.

[3] P. Vecer, M. Kreidl and R. Smid. "Condition indicators for gearbox condition monitoring systems". Acta Polytechnica. Vol. 45, pp. 35-43. 2005.

[4] P.D. Samuel and D.A. Pines. "A review of vibration-based techniques for helicopter transmission diagnostics". Journal of Sound and Vibration. Vol. 282, pp. 475-508. 2005.

[5] T. Barszcs and R.B. Randall. "Application of spectral kurtosis for detection of a tooth crack in the planetary gear of a wind turbine". Mechanical Systems and Signal Processing. Vol. 23, pp. 1352-1365. 2009.

[6] J. Keller and P. Grabill. "Vibration monitoring of UH-60A main transmission planetary carrier fault". American Helicopter Society. 59th Annual Forum. 2003.

[7] P. McFadden and J. Smith. "An explanation for the asymmetry of the modulation sidebands about the tooth meshing frequency in epicyclic gear vibration". Proceedings of the Institution of Mechanical Engineers. 199(C1), pp. 65-70. 1985.

[8] S. Harris. "Dynamic loads on the teeth of spur gears". Proceedings of the Institution of Mechanical Engineering. Vol. 172, pp. 87-112. 1958.

[9] D. Basset and D. Houser. "The design and analysis of single flank transmission error tester for loaded gears". NASA Contractor Report Nº 179621. 1987.

[10] M. Inalpolat and A. Kahraman. "A theoretical and experimental investigation of modulation sidebands of planetary gear sets". Journal of Sound and Vibration. Vol. 323, Issues 3-5, pp. 677-696. 2009.

[11] C. Molina Vicuña. "Contributions to the analysis of vibrations and acoustic emissions for the condition monitoring of epicyclic gearboxes". RWTH Aachen University. 2010.

[12] R.G. Parker and J. Lin. "Mesh phasing relationships in planetary and epicyclic gears". Journal of Mechanical Design. Vol. 126, Issue 2, pp. 365-370. 2004.

[13] J. McNames. "Fourier Series Analysis of Epicyclic Gearbox Vibration". Journal of Vibration and Acoustics. Vol. 124, pp. 150-152. 2002.

[14] S. Sheng. "Wind Turbine Gearbox Condition Monitoring Round Robin Study-Vibration Analysis". Technical Report NREL/TP-5000-54530. 2012.

[15] Z. Feng and M.J. Zuo. "Vibration signal models for fault diagnosis of planetary gearboxes". Journal of Sound and Vibration. Vol. 331, pp. 4919-4939. 2012.

[16] H. Luo, Ch. Hatch, J. Hanna, M. Kalb, A. Weiss, J. Winterton, M. Inalpolat and C. Dannehy. "Amplitude modulations in planetary gears". Wind Energy. DOI: 10.1002/we.1545. 2012.